Microstructure effects on the lower critical solution temperature phase behavior of deuterated polybutadiene and protonated polyisoprene blends studied by small-angle neutron scatt...

5 AUTHORS, INCLUDING:

Hiroshi Jinnai
Tohoku University
234 PUBLICATIONS **4,217** CITATIONS

SEE PROFILE

Hirokazu Hasegawa
Kyoto University
163 PUBLICATIONS **4,887** CITATIONS

SEE PROFILE

Takeji Hashimoto
Kyoto University
516 PUBLICATIONS **16,947** CITATIONS

SEE PROFILE

Microstructure Effects on the Lower Critical Solution Temperature Phase Behavior of Deuterated Polybutadiene and Protonated Polyisoprene Blends Studied by Small-Angle Neutron Scattering

Shinichi Sakurai,[†] Hiroshi Jinnai, Hirokazu Hasegawa, and Takeji Hashimoto*

Department of Polymer Chemistry, Faculty of Engineering, Kyoto University, Sakyo-ku, Kyoto 606, Japan

Charles C. Han

Polymers Division, National Institute of Standards and Technology, Gaithersburg, Maryland 20899

ABSTRACT: The miscibility of a blend of protonated polyisoprene (HPI) with the 3,4-linkage microstructure in the range 7–15% and of deuterated polybutadiene (DPB) with the 1,2-linkage microstructure in the range 12–28% was studied by small-angle neutron scattering (SANS). It was found that all blends studied here show lower critical solution temperature (LCST) type phase behaviors; i.e., the phase separation occurs by raising the temperature. It was also found that the miscibility is quite sensitive to the microstructures of the polydienes used. The effective thermodynamic interaction parameter χ_{eff} per segment between two polymers was determined by fitting SANS data in the single-phase state with a theoretical scattering curve obtained on the basis of the random-phase approximation. The temperature dependence of χ_{eff} showed a systematic change with the microstructure. For a given HPI, the χ_{eff} values decreased, and therefore, the blends became more miscible, with an increase in the vinyl content (i.e., 1,2-linkage content) in DPB. On the contrary, for a given DPB, the values increased, and therefore, the blends became more immiscible, with an increase in the vinyl content (i.e., 3,4-linkage content) in HPI. We proposed an alternative explanation for the LCST phase behavior based on treatment for the random copolymer blends.

I. Introduction

The miscibility of binary polymer mixtures has been studied intensively because of interests both from academic and technological points of view.[1-9] A relationship between the miscibility and the primary structures of the polymers involved is specially interesting. It has been found that the miscibility depends on the microstructure[3,4] (the geometrical isomers) for blends of polydiene, tacticity[5,6] for vinyl polymers, and deuterium labeling,[7-10] which is necessary for small-angle neutron scattering (SANS) to attain scattering contrast. For control of the miscibility and molecular design of a blend system, it is necessary to study systematically these effects, in addition to the dependence of molecular weight and blend composition. In order to separate out these effects from molecular weight and blend composition, it is useful to evaluate the Flory interaction parameter χ, which can be obtained by analyzing a scattering function obtained from a homogeneous mixture in the single-phase state. For this purpose, the SANS technique is often used.[2-4,7-11] Then one can predict the thermodynamic stability limit of a given mixture in terms of χ at the spinodal point, χ_S, which is a function of the molecular weights and the blend compositions of constituent polymers.

We have been studying the microstructure and the deuterium labeling effects on the blend miscibility using well-characterized polydienes as model polymers. In our earlier paper,[3] the microstructure and the isotopic labeling effects of deuterated and protonated polybutadiene (DPB/HPB) blends were discussed in terms of the idea of the random copolymer blend.[12-14]

† Present address: Department of Polymer Science and Engineering, Kyoto Institute of Technology, Matsugasaki, Sakyo-ku, Kyoto 606, Japan.

The aim of this paper is to investigate the microstructure effects on the miscibility of deuterated polybutadiene/protonated polyisoprene (DPB/HPI) blends in terms of χ by using the well-characterized polymers DPB and HPI. We have shown some obvious evidence of the lower critical solution temperature (LCST) phase behavior of the DPB/HPI blend system by SANS and time-resolved light scattering (LS) in a previous paper.[15] The LCST phase behavior is generally explained by the existence of a specific interaction, for example, in the case of the polystyrene/poly(vinyl methyl ether) (PS/PVME) blend system.[16] Here we propose another possibility for the blend system to have the LCST type phase diagram, in terms of the idea of the random copolymer blend[12-14] as a result of a subtle balance of the constituent fundamental interactions. The molecular weight effect on χ was not specifically studied in this paper. However, we expect the effect is small for the high molecular weight polymers covered in this work.

II. Experimental Section

The polydiene samples were synthesized by living anionic polymerization initiated by *sec*-butyllithium and have narrow molecular weight distributions. Characterization data are listed in Table I where the sample code (e.g., HPI-7-101) comprises the kind of polymer (HPI), the vinyl content in % (the first number, 7 in this case), and the weight-average molecular weight, M_w, in units of 1000 (the second number, 101 in this case). Three HPI samples were synthesized in xylene and have microstructures with contents of 3,4-linkage in the range 7–15%. Four DPB samples were synthesized in benzene and have microstructures with contents of 1,2-linkage in the range 12–28%. The characterization of the microstructure were performed by ^{13}C NMR,[17,18] and the molecular weight and the polydispersity were obtained by GPC with a light-scattering photometer, except for DPB-12-52, in which the number-average molecular weight, M_n, and the heterogeneity index, M_w/M_n, were obtained by membrane

osmometry and GPC, respectively. None of the polydienes used in this study has measurable crystallinity. The samples coded HPI-7-101 and DPB-12-52 are identical with GL-4 and H-9 in our previous paper,[15] respectively.

The SANS measurements were carried out at the research reactor of the National Institute of Standards and Technology.[19] Detailed experimental methods as well as SANS data reduction procedures were described elsewhere.[3]

III. Results and Discussion

(A) LCST Phase Behaviors. Similar LCST type phase behaviors as reported for GL-4/H-9 in ref 15 were observed for the temperature dependence of the SANS profile, $S(q)$ (in unit of cm^{-1}) vs q, for all 10 pairs of DPB and HPI studied. These 10 pairs are combinations of DPB and HPI listed in Table I except for HPI-12-192/DPB-12-52 and HPI-15-136/DPB-12-52. $S(q)$ denotes the scattered intensity observed at q where q is the magnitude of the scattering vector given by $q = (4\pi/\lambda) \sin (\theta/2)$, λ and θ being the wavelength of the neutron (=9 Å used) and the scattering angle, respectively. The scattered intensity at all q's increases with increasing temperature, T, below the cloud-point temperature, $T_{C,SANS}$, indicating that the thermal concentration fluctuation is enhanced with increasing T. Above $T_{C,SANS}$, the scattered intensity is found to be time-dependent, suggesting that phase separation occurred.

Using a nonlinear regression fitting routine,[7] all SANS profiles $S(q)$ were fitted with a generalized version[7,20] of the scattering theory of de Gennes[11] based on the random-phase approximation (RPA) for a mixture of polydispersed polymers with asymmetry in the segment size

$$S(q)_{RPA} = k_N \Big/ \left[\frac{1}{\phi_A \langle z_A \rangle_n \upsilon_A S_A(q)} + \frac{1}{\phi_B \langle z_B \rangle_n \upsilon_B S_B(q)} - \frac{2\chi}{\upsilon_0} \right] \quad (1)$$

with $S(q) = S(q)_{RPA}$ + baseline where $S(q)_{RPA}$ denotes the theoretical structure factor based on the RPA. χ is the Flory interaction parameter between DPB and HPI per segment. $S_K(q)$ denotes the scattering function of the Gaussian chain for the Kth component with the effect of polydispersity,[3] i.e.,

$$S_K(q) \equiv \frac{2}{(q^2 \langle R_{gK}^2 \rangle)^2} \left[q^2 \langle R_{gK}^2 \rangle - 1 + \left(\frac{h_K}{h_K + q^2 \langle R_{gK}^2 \rangle} \right)^{h_K} \right] \quad (2)$$

where $\langle R_{gK}^2 \rangle$ ($\equiv \langle z_K \rangle_n b_K^2/6$) is the mean square radius of gyration of the Kth component with $\langle z_K \rangle_n$ and b_K being the number-average degree of polymerization (DP) and the Kuhn statistical segment length for the Kth component. h_K is defined by $h_K \equiv 1/(\langle z_K \rangle_w/\langle z_K \rangle_n - 1)$ which relates to the heterogeneity index, with $\langle z_K \rangle_w$ being the weight-average DP. ϕ_K and υ_K denote a volume fraction and a segment molar volume for the Kth component, respectively, and υ_0 denotes the reference cell volume.

The SANS profile obtained in the single-phase state could be fitted very nicely with eq 1, as shown previously.[3,15] It is important to point out an estimation error for the determination of the χ value, since the microstructure effect will be discussed in terms of χ later in subsection B. The error encountered in the fitting analysis by means of eq 1 is normally negligibly small compared with that due to a measurement error of the molecular weight. We estimate an error of ±5% for the molecular weight

Table I
Sample Characteristics[a,c]

Protonated Polyisoprene (HPI)						
			microstructure, %			
sample	$10^{-3}M_n$	M_w/M_n	3,4	cis-1,4	trans-1,4	1,2
HPI-7-101	100	1.0_1	7	69	24	0
HPI-12-192	192	1.0_1	12	66	22	0
HPI-15-136	136	1.0_1	15	63	22	0

Deuterated Polybutadiene (DPB)					
			microstructure, %		
sample	$10^{-3}M_n$	M_w/M_n	1,2	cis-1,4	trans-1,4
DPB-12-52[b]	49	1.0_7	12	36	52
DPB-16-61	59	1.0_3	16	38	46
DPB-20-103	103	1.0_1	20	36	44
DPB-28-71	71	1.0_1	28	27	45

[a] M_n and M_w were determined by GPC with a light-scattering photometer. [b] M_n and M_w/M_n of DPB-12-52 were determined by membrane osmometry and by GPC, respectively. [c] Microstructures were determined by ^{13}C NMR.

measurement, which causes an error of approximately 1.8×10^{-4} for χ.

The thermodynamic interaction parameter per segment thus determined for the HPI/DPB blends should only be considered as an effective χ value (χ_{eff}) in the following discussion, simply because the monomers comprise different microstructures and the monomer/monomer interaction depends on these microstructures. Since polymer/polymer blends can be described by the mean-field theory,[2,21-24] the spinodal temperature, T_S, can be obtained by an extrapolation of χ_{eff} to χ_S, at which $S(q=0)^{-1}$ goes to zero, or ξ^{-2} goes to zero, in a plot of χ_{eff} vs T^{-1}, $S(q=0)^{-1}$ vs T^{-1}, or ξ^{-2} vs T^{-1}, respectively, where χ_S is given by

$$\chi_S = \frac{\upsilon_0}{2} \left[\frac{1}{\phi_A \langle z_A \rangle_w \upsilon_A} + \frac{1}{\phi_B \langle z_B \rangle_w \upsilon_B} \right] \quad (3)$$

and characterizes the stability limit of the mixture. $S(q=0)$ is the zero-wavenumber structure factor, and ξ is the correlation length. Now let us estimate the error in determining T_S. As shown above, the χ_{eff} value may contain the error of the order of 1.8×10^{-4} owing to the error of the molecular weight measurement. Since the error of the molecular weight measurement affects χ_S and χ_{eff} in the same way and by the same magnitude, the effects of these errors in χ_S and χ_{eff} on T_S may be cancelled, and therefore, the T_S thus estimated may be considerably accurate. Typical plots of χ_{eff} vs T^{-1}, $S(q=0)^{-1}$ vs T^{-1}, and ξ^{-2} vs T^{-1}, which allow us to determine T_S, are shown in our previous work (see Figure 4a-c in ref 15).

Phase diagrams obtained for the blends of HPI-7-101 with various DPB's are shown in Figure 1. The symbols, circles, triangles, and squares, indicate thus obtained T_S, $T_{C,SANS}$, and $T_{C,LS}$, respectively. $T_{C,SANS}$ and $T_{C,LS}$ are the cloud-point temperatures determined by SANS and LS, respectively. The procedure for determining these temperatures has been described in our previous work.[15] For the HPI-7-101/DPB-28-71 system, the cloud-point temperatures were not observed because the phase separation did not actually occur up to 200 °C, and the polymers were thermally unstable above 200 °C. Note that the determination of T_S involving the long extrapolation was not very accurate for this particular blend system. In each part of Figure 1, the calculated critical composition, ϕ_C, is also indicated by an arrow, where $\phi_{C,A}$
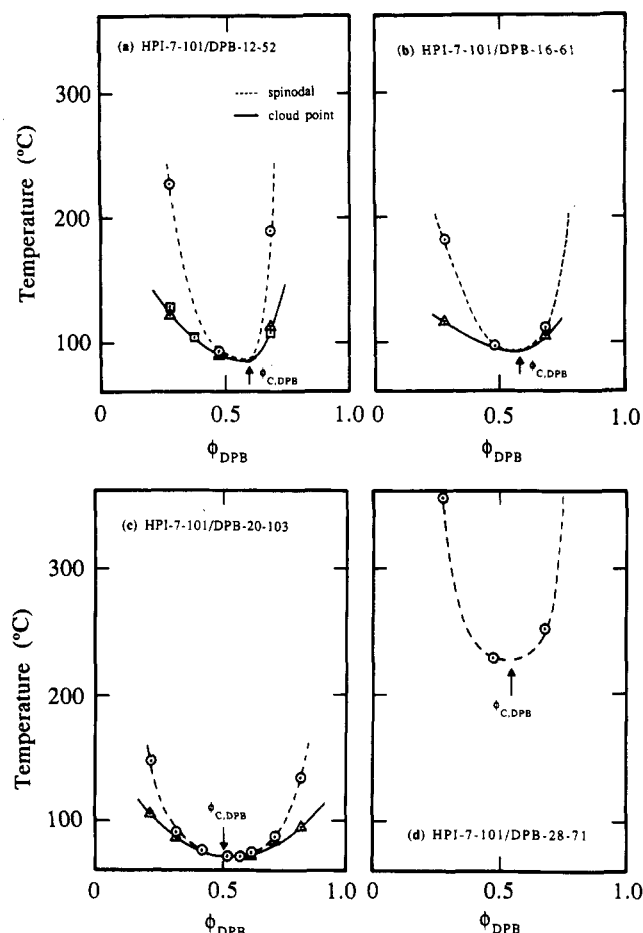
Figure 1. Phase diagrams of blends for HPI-7-101 with (a) DPB-12-52, (b) DPB-16-61, (c) DPB-20-103, and (d) DPB-28-71. The spinodal temperature T_S determined by SANS, the cloud-point temperature by SANS $T_{C,SANS}$, and that by LS $T_{C,LS}$ are shown, respectively, by circles, triangles, and squares. Arrows show calculated $\phi_{C,DPB}$ by eq 4 in the text.

is given by [15,16]

$$\phi_{C,A} = \frac{\left(\dfrac{\upsilon_B \langle z_B \rangle_w}{\langle z_B \rangle_z / \langle z_B \rangle_w}\right)^{1/2}}{\left(\dfrac{\upsilon_A \langle z_A \rangle_w}{\langle z_A \rangle_z / \langle z_A \rangle_w}\right)^{1/2} + \left(\dfrac{\upsilon_B \langle z_B \rangle_w}{\langle z_B \rangle_z / \langle z_B \rangle_w}\right)^{1/2}} \quad (4)$$

where $\langle z_K \rangle_z$ is the z-average DP for the Kth component. Assuming the Shultz–Zimm distribution function for the polydispersity, $\langle z_K \rangle_z / \langle z_K \rangle_w$ can be written[3] by $(h_K + 2)/(h_K + 1)$. It is obvious that all the blends have the LCST type phase diagrams, and the blend miscibility is likely affected not only by the molecular weights but also by the microstructures of these DPB's. One can obviously see the effect of microstructures by comparing parts a, b, and d in Figure 1. Although the molecular weight of the DPB for Figure 1d is similar or slightly higher than that of the DPB for Figure 1a or for Figure 1b, the miscible region in the phase diagram shown in Figure 1d is much wider than that shown in Figure 1a or in Figure 1b, respectively. We will now discuss the microstructure effect on the blend miscibility in terms of χ_{eff}.

(B) Microstructure Effects on Blend Miscibility. In order to discuss the microstructure effects on the blend miscibility, the χ_{eff}'s for each HPI/DPB blend at a given blend composition should be compared. All χ_{eff} values measured at $\phi_{DPB} = 0.475$ are plotted against T^{-1} in Figure 2. There are 10 sets of data on χ_{eff}, which are shown in two parts: part a shows the effect of the DPB microstruc-
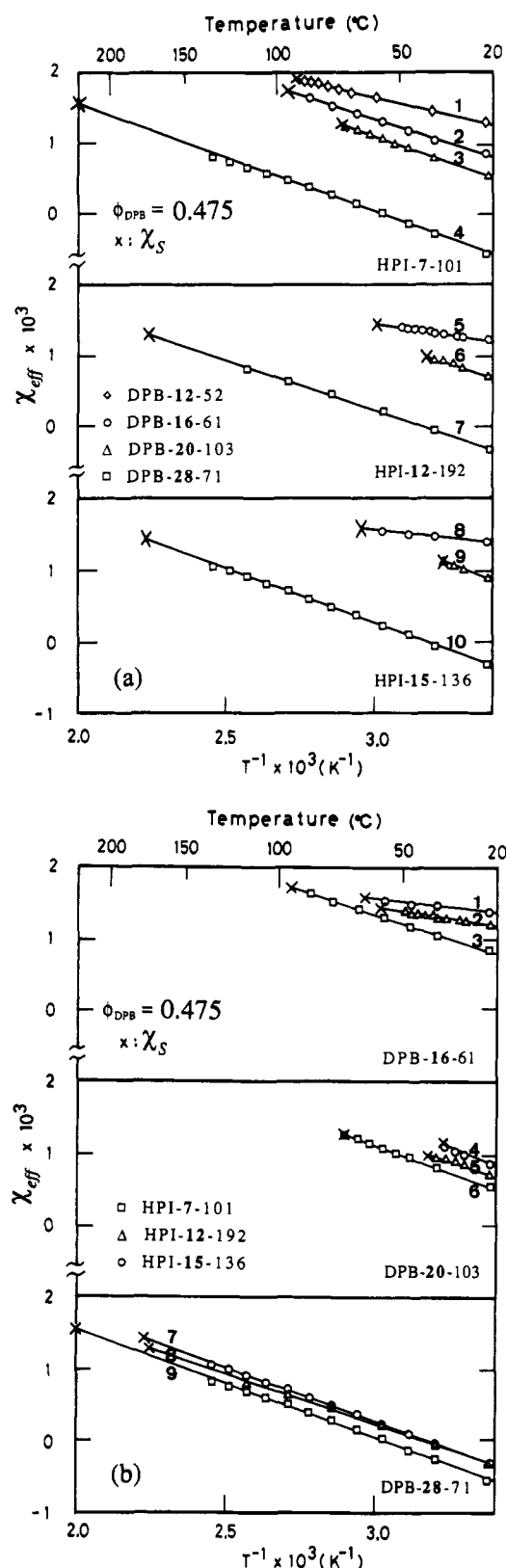
Figure 2. (a) χ_{eff} plotted as a function of T^{-1} for blends of HPI-7-101 with (1) DPB-12-52, (2) DPB-16-61, (3) DPB-20-103, and (4) DPB-28-71, for blends of HPI-12-192 with (5) DPB-16-61, (6) DPB-20-103, and (7) DPB-28-71, and for blends of HPI-15-136 with (8) DPB-16-61, (9) DPB-20-103, and (10) DPB-28-71. The composition of each blend is fixed at $\phi_{DPB} = 0.475$. (b) χ_{eff} plotted as a function of T^{-1} for blends of DPB-16-61 with (1) HPI-15-136, (2) HPI-12-192, and (3) HPI-7-101, for blends of DPB-20-103 with (4) HPI-15-136, (5) HPI-12-192, and (6) HPI-7-101, and for blends of DPB-28-71 with (7) HPI-15-136, (8) HPI-12-192, and (9) HPI-7-101. The composition of each blend is fixed at $\phi_{DPB} = 0.475$.

Table II
$A(x, y)$ and $B(x, y)$ for the HPI/DPB System

system[a]	x	y	$A(x, y)$	$B(x, y)$	χ_s	T_s, °C
1	0.07	0.12	4.62×10^{-3}	-0.989	1.91×10^{-3}	92
2	0.07	0.16	5.34×10^{-3}	-1.33	1.73×10^{-3}	95
3	0.07	0.20	5.51×10^{-3}	-1.47	1.26×10^{-3}	73
4	0.07	0.28	4.58×10^{-3}	-1.51	1.57×10^{-3}	229
5	0.12	0.16	3.42×10^{-3}	-0.655	1.45×10^{-3}	59
6	0.12	0.20	5.31×10^{-3}	-1.36	0.99×10^{-3}	42
7	0.12	0.28	4.43×10^{-3}	-1.40	1.30×10^{-3}	174
8	0.15	0.16	2.96×10^{-3}	-0.466	1.58×10^{-3}	65
9	0.15	0.20	6.22×10^{-3}	-1.58	1.11×10^{-3}	36
10	0.15	0.28	4.78×10^{-3}	-1.51	1.42×10^{-3}	176

[a] See the legend for the identification numbers in Figure 2a.

ture on χ_{eff} for three given HPI's, and part b shows the effect of the HPI microstructure on χ_{eff} for three given DPB's. As discussed above, the error in the χ_{eff} values may be within ca. 1.8×10^{-4}; one can consider an error bar of double the size of each symbol in Figure 2. It is clear that all the χ_{eff} values show a linear relationship with T^{-1}, i.e.,

$$\chi_{eff} = A + B/T \tag{5a}$$

with a negative slope ($B < 0$) for each blend system. This indicates that all the HPI/DPB blends studied here have the LCST type phase behavior, irrespective of the microstructures covered in our experiment. At a given temperature, it can be seen that the value χ_{eff} decreases as the content of vinyl linkage (i.e., 1,2-linkage) in DPB increases. On the contrary, the value increases as the content of vinyl linkage (i.e., 3,4-linkage) in HPI increases, indicating that the blend becomes more miscible by increasing the vinyl content of DPB or by decreasing the vinyl content of HPI. It is quite interesting to note that the pure microstructure effect of DPB and that of HPI on χ_{eff} are quite opposite to each other. However, if we examine more closely the temperature dependencies of χ_{eff}, for example, systems 8 and 9 in Figure 2a, one may expect a crossing at around 60 °C by an extrapolation of the data for system 9, indicating that the degree of miscibility may be inverted at higher temperatures. Therefore, it is worth expressing the temperature dependencies of χ_{eff} as a function of the content of the microstructure for HPI and that for DPB:

$$\chi_{eff}(x, y) = A(x, y) + B(x, y)/T \tag{5b}$$

where x and y are the volume fraction of 3,4-linkage in HPI and that of 1,2-linkage in DPB, respectively. The results are listed in Table II.

It is important to note here that the effect of the microstructure on χ_{eff} is rather small, not at all striking, and of the order of 10^{-3}. However, this small change of the interaction parameter cannot be ignored but rather becomes increasingly important as the molecular weights of polymers increase. This is clear from eq 3, because the value of χ_s itself becomes a small quantity, of the order of 10^{-3} or even smaller, with increasing the weight-average DP's, $\langle z_A \rangle_w$ and $\langle z_B \rangle_w$. In other words, the stability limit is determined by the net interaction parameter between the two polymers, i.e., χ_{eff} times DP. If DP is large, a **small change of the value of** χ_{eff} due to the small change in the primary structure of polymers causes **a strikingly large effect** on the stability limit and hence on the miscibility (**a large cooperative effect**).

χ_{eff} is negative at low temperatures and positive at high temperatures, implying the net attractive and repulsive interactions at low and high temperatures, respectively. It is also worth noting that the microstructure affects the *entropic part* of χ_{eff}, i.e., $A(x, y)$, more dominantly than the *enthalpic part*, i.e, $B(x, y)$.

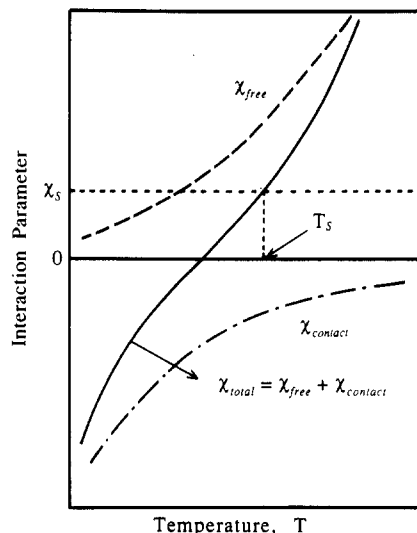**Figure 3.** Illustration giving a general explanation for the LCST type phase behavior in terms of χ_{free} and $\chi_{contact}$ where χ_{free} and $\chi_{contact}$ denote a contribution to the net χ_{total} due to a free volume change and that due to a contact energy change, respectively. T_s denotes the spinodal temperature and χ_s is the χ value at $T = T_s$.
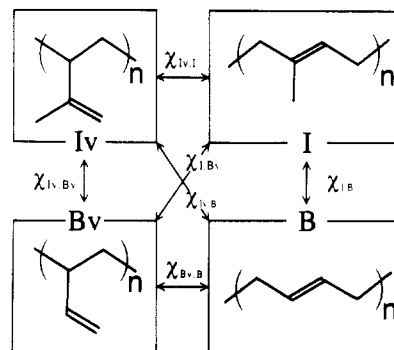

Figure 4. Schematic representation for notations of the fundamental binary interaction parameter χ's between two different microstructures of HPI and DPB.

(C) Explanation for the LCST-Type Phase Behavior of HPI/DPB Blends. The net interaction parameter per segment between two polymers comprises the contribution (i) of the free volume change (χ_{free}) and (ii) of a contact energy change ($\chi_{contact}$) upon mixing.[25,26] These contributions are sketched in Figure 3, where the interaction parameter is shown as a function of T. As a result of a large contribution of the positive χ_{free} at high temperature and that of the negative $\chi_{contact}$ at low temperature due to a specific group interaction, $\chi(=\chi_{free} + \chi_{contact})$ increases with increase of temperature (LCST type). However, it is difficult to consider such an attractive interaction in the case of the HPI/DPB blend because of the similarity between isoprene and butadiene monomers. It is also difficult to consider such a large χ_{free} as that found in PS/PVME,[7] because of a possible similarity of the *PVT* relationships between DPB and HPI. Then we try to take the idea of the random copolymer blend as an alternative interpretation of the LCST type phase behavior.

As shown in Figure 4, we assume that HPI is a random copolymer comprising the 3,4-linkage (Iv) and the 1,4-linkage (I) and also that DPB is a random copolymer comprising the 1,2-linkage (Bv) and the 1,4-linkage (B), by neglecting tacticity and the difference between cis-1,4 and trans-1,4. Then the χ_{eff} value as a function of x and y is given by six sets of the fundamental χ's as follows:
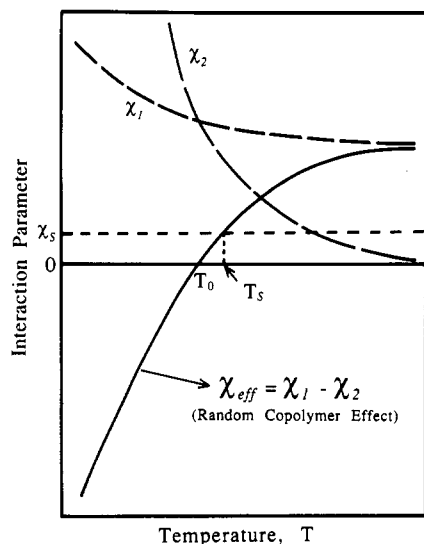
Figure 5. Illustration demonstrating an alternative explanation for the LCST type phase behavior caused by a subtle balance of the UCST type fundamental χ's. χ_{eff} is given by $\chi_1 - \chi_2$ where χ_1 and χ_2 are *inter*- and *intra*molecular interactions, respectively. χ_1 is equal to χ_2 at $T = T_0$.

$$\chi_{\text{eff}}(x, y) = \chi_1 - \chi_2 \tag{6a}$$

$$\chi_1 = xy\chi_{\text{Iv,Bv}} + x(1 - y)\chi_{\text{Iv,B}} + (1 - x)y\chi_{\text{I,Bv}} + (1 - x)(1 - y)\chi_{\text{I,B}} \tag{6b}$$

$$\chi_2 = x(1 - x)\chi_{\text{Iv,I}} + y(1 - y)\chi_{\text{Bv,B}} \tag{6c}$$

where $\chi_{i,j}$ denotes the fundamental χ between i and j segments (i, j = Iv, I, Bv, or B), and χ_1 and χ_2 denote the contributions of *inter*- and *intra*-molecular interactions. It should be noticed that the intramolecular interaction contributes negatively to the net interaction χ_{eff}. This means that the greater is the repulsive interaction between different types of segment within a random copolymer chain, the more miscible is the copolymer with any other polymer.

Since we have a total of 10 experimental data sets of χ_{eff} as shown in Figure 2a, 10 simultaneous equations in the form of eqs 6a–6c can be obtained, using the data of $A(x, y)$ and $B(x, y)$, as listed in Table II. To get all the fundamental χ's as a function of temperature ($\chi = A + B/T$), the simultaneous equations should be solved. However, the evaluations of the fundamental χ's seem impossible in a rigorous sense because the values of x and y are experimentally varied only in a limited range ($0.07 \leq x \leq 0.15$ and $0.12 \leq y \leq 0.28$) and hence even a small measurement error in these values may crucially affect solutions of the simultaneous equations. Moreover, the small number of degrees of freedom in the analysis (10 sets of data and 6 sets of parameters) may reduce the validity of the evaluated sets of the fundamental χ's. More experimental examinations should be desired. Therefore, we will show only qualitative explanation of the LCST type phase behavior based on the random copolymer effect.

The LCST type phase behavior for the HPI/DPB blends studied here may be interpreted as sketched in Figure 5, where χ_1 and χ_2 are, respectively, defined by eqs 6b and 6c, corresponding to the inter- and intra-molecular contributions to the net value χ_{eff}. Even in the particular

case in which all fundamental binary interactions between any two different microstructures decrease with increase of temperature, i.e., UCST type, giving rise to decreasing χ_1 and χ_2, with increasing temperature, the temperature dependencies of χ_1 and χ_2 are conceivably given as shown in Figure 5, i.e., $\chi_1 < \chi_2$ for $T < T_0$, $\chi_1 > \chi_2$ for $T > T_0$, and $\chi_1 = \chi_2$ for $T = T_0$. Such a subtle balance of the UCST type *inter*- and *intra*molecular interactions may give rise to the net LCST type phase behavior on the temperature dependence of χ_{eff}, i.e., the net attractive interactions at low temperatures and repulsive interactions at high temperatures. It should be noted here that absolute values of χ_1 and χ_2 are immaterial, but only the relative values of them are significant.

References and Notes

(1) Paul, D. R., Newman, S., Eds. *Polymer Blends*; Academic Press: New York, 1978.
(2) Han, C. C.; Bauer, B. J.; Clark, J. C.; Muroga, Y.; Matsushita, M.; Okada, M.; Tran-Cong, Q.; Chang, T.; Sanchez, I. C. *Polymer* **1988**, *29*, 2002.
(3) Sakurai, S.; Hasegawa, H.; Hashimoto, T.; Glen Hargis, I.; Aggarwal, S. L.; Han, C. C. *Macromolecules* **1990**, *23*, 451.
(4) Sakurai, S.; Izumitani, T.; Hasegawa, H.; Hashimoto, T.; Han, C. C. *Macromolecules*, in press.
(5) Trask, C. A.; Roland, C. M. *Macromolecules* **1989**, *22*, 256.
(6) Beaucage, G.; Stein, R. S.; Hashimoto, T.; Hasegawa, H. *Macromolecules* **1991**, *24*, 3443.
(7) Shibayama, M.; Yang, H.; Stein, R. S.; Han, C. C. *Macromolecules* **1985**, *18*, 2179.
(8) Yang, H.; Shibayama, M.; Stein, R. S.; Shimizu, N.; Hashimoto, T. *Macromolecules* **1986**, *19*, 1667.
(9) Yang, H.; Stein, R. S.; Han, C. C.; Bauer, B. J.; Kramer, E. J. *Polymer Commun.* **1986**, *27*, 132.
(10) Bates, F. S.; Wignall, G. D. *Phys. Rev. Lett.* **1986**, *57*, 1429.
(11) de Gennes, P.-G. *Scaling Concepts in Polymer Physics*; Cornell University Press: Ithaca, NY, 1979.
(12) ten Brinke, G.; Karasz, F. E.; MacKnight, W. J. *Macromolecules* **1983**, *16*, 1827.
(13) Kambour, R. P.; Bendler, J. T.; Bopp, R. C. *Macromolecules* **1983**, *16*, 753.
(14) Paul, D. R.; Barlow, J. W. *Polymer* **1984**, *25*, 487.
(15) Hasegawa, H.; Sakurai, S.; Takenaka, M.; Hashimoto, T.; Han, C. C. *Macromolecules* **1991**, *24*, 1813.
(16) Nishi, T.; Kwei, T. K. *Polymer* **1975**, *16*, 285.
(17) Sato, H.; Takebayashi, K.; Tanaka, Y. *Macromolecules* **1987**, *20*, 2418.
(18) Sato, H.; Ono, A.; Tanaka, Y. *Polymer* **1977**, *18*, 580.
(19) Glinka, C. J.; Rowe, J. M.; LaRock, J. G. *J. Appl. Cryst.* **1986**, *19*, 427.
(20) Warner, M.; Higgins, J. S.; Carter, A. J. *Macromolecules* **1983**, *16*, 1931.
(21) Joanny, J. F. *J. Phys. A* **1978**, *11*, L117.
(22) de Gennes, P.-G. *J. Phys. Lett.* **1977**, *38*, L441.
(23) Binder, K. *J. Chem. Phys.* **1983**, *79*, 6387.
(24) Han, C. C. In *Molecular Conformation and Dynamics of Macromolecules in Condensed Systems*; Nagasawa, M., Ed.; Elsevier: New York, 1988.
(25) Patterson, D. *Macromolecules* **1969**, *2*, 672.
(26) Sanchez, I.; Lacombe, R. H. *J. Phys. Chem.* **1976**, *80*, 2352; **1976**, *80*, 2568.